PERGAMON

European Journal of Cancer 38 (2002) 2116–2127

European Journal of Cancer

www.ejconline.com

Functional MRI for anticancer therapy assessment

A.R. Padhani*

Paul Strickland Scanner Centre, Mount Vernon Hospital, Rickmansworth Road, Northwood, Middlesex HA6 2RN, UK

Received 18 October 2001; accepted 10 December 2001

Abstract

Anticancer drug discovery and development are experiencing a paradigm shift from cytotoxic therapies to more selective therapies that target underlying oncogenic abnormalities. Many newer therapies are cytostatic, for which objective tumour shrinkage is an inappropriate response parameter. There is a growing need to develop surrogate endpoints of drug efficacy to speed up the process of finding effective drug combinations for phase III trials. This review focuses on the developing field of functional magnetic resonance imaging (MRI) and its potential applications in the pharmacodynamic evaluation of existing and new cancer therapeutics. Dynamic contrast enhanced MRI, which is currently being used to evaluate anti-angiogenic, and anti-vascular agents in human trials will be reviewed in detail. The requirements that must be met before incorporating functional MRI techniques into clinical protocols are also discussed.

Keywords: Magnetic resonance imaging; Tumour; Angiogenesis; Treatment response

1. Introduction

Monitoring the response of tumours to treatment is an integral and increasingly important function of radiologists working in oncological imaging. Imaging studies allow an objective method of quantifying tumour response to a variety of physical and pharmaceutical treatments. Objective tumour shrinkage has been widely adopted as a standard endpoint to select new anticancer drugs for further study, as a prospective endpoint for definitive clinical trials designed to estimate the benefit of treatment in a specific group of patients, and is widely used in everyday clinical practice to guide clinical decision-making. Standard size criteria for measuring therapeutic response were first proposed in 1981 and, although they have been adapted by various cancer organisations, they continue to be used largely unchanged [1–3]. Recently, the World Heath Organization (WHO), the National Cancer Institute (NCI) and the European Organization for Research and Treatment of Cancer (EORTC) have adopted a new set of tumour response size criteria (Response Evaluation Criteria in Solid Tumours—RECIST) [4].

There are many recognised limitations of size change as a tumour response variable. Size changes for both response and progression are arbitrary and traditionally expressed as a percentage change from baseline. There are numerous errors in obtaining tumour measurements. These arise from observer variations on the estimated position of the boundary of lesions. The edges of irregular or infiltrating lesions are often difficult to identify and indeed, some tumours are impossible to measure, for example, pulmonary lymphangitis carcinomatosa and ovarian carcinoma seeding into the peritoneal space. So serious are measurement errors, that 'independent review panels' are often employed by pharmaceutical companies to standardise response assessments in clinical trials. Independent review panels can disagree with 'home radiologists' in 50% of cases with major disagreements occurring in up to 40% of cases [5]. A change in size may also be delayed chronologically, often requiring several treatments before a decision can be made on whether a treatment is effective. Reports from the functional imaging literature, particularly positron emission tomography (PET) suggest that metabolic and physiological changes antecede size change [6]. For example, in patients with lymphoma responding to treatment, changes in energetics can be detected by 18-(FDG)-PET within hours [7] whilst

* Tel.: +44-1923-844-353; fax: +44-1923-844-600.
E-mail address: anwar@padhani.fsnet.co.uk (A.R. Padhani).

0959-8049/02/$ - see front matter
PII: S0959-8049(02)00388-X

morphological changes are delayed in their appearance. Size changes may also fail to correspond to the patient's clinical condition. All of us have observed patients in whom there is obvious clinical progression (for example, deterioration of performance status, haematological indices and tumour markers) with no change in the size of marker lesions. Similarly, clinically inactive disease may be present with enlarging lesions, particularly in patients with non-seminomatous germ cell tumours [8]. As a result, there is currently a pressing need to develop additional response parameters to overcome these limitations, and to address the growing need to monitor the response to treatment of a new generation of selective anticancer drugs. Cytotoxic chemotherapy is usually directed at molecular targets present in both normal and tumour tissues, and therefore toxicity to normal tissues limits this approach. Recent molecular understanding of the processes of tumour development and metastasis has lead to the identification of new targets for potential anticancer treatments. These targets are involved at one level or more in tumour biology, including tumour cell proliferation and invasion, angiogenesis and metastasis. Imaging studies may provide early evidence of drug activity sometimes directed at the site of biological action. These may then be used as surrogate endpoints of drug efficacy to speed up the process of finding more effective drug combinations to enter into phase III trials.

So where should we look for new imaging response parameters? The clues are already here in what we can measure today and in new molecular imaging technologies [9]. Functional imaging parameters that reflect tumour vascularity, microenvironment and cell metabolism should be investigated as tumour response variables. These tumour features are inextricably linked in the majority of solid tumours [10,11]. Although the transition of dormant to active vascularisation is not fully understood, it is clear that the metabolic microenvironment of tumours plays an essential role. Important metabolic factors include oxygenation, pH, metabolic and energetic status, and interstitial pressure and transport. These microenvironmental factors also have a direct effect on tumour cellular processes including gene expression and tumour proliferation, metastatic potential, and sensitivity to radiotherapy and anticancer drugs [12,13]. A variety of imaging techniques that assess cellular metabolic processes may act as tumour response variables. For example, 18-FDG-PET and 11-C-thymidine PET reflect on glucose metabolism and the proliferative activity of tumours [14] and 31-P-magnetic resonance (MR) spectroscopy and 1-H-MRS enable cellular energetics and membrane turnover to be assessed [15]. Dynamic contrast medium enhanced (DCE-magnetic resonance imaging (MRI)) which provides insights concerning tumour perfusion, capillary permeability and leakage space is discussed in detail in this article [16]. Other MR techniques are able to measure intracellular pH (31-P-MRS), water diffusion and cell membrane integrity (diffusion imaging) [17]. The development of novel contrast agents will enable the distribution of extracellular pH to be mapped and 18-fluoromidonidazole can be used as a PET imaging agent to measure tumour hypoxia non-invasively [18]. Furthermore, molecular imaging techniques currently being developed will enable us to image processes such as intracellular signalling, imaging of gene delivery and expression, and imaging of drug delivery [19].

2. Imaging angiogenic targeted treatments

Functional characterisation of the tumour neovasculature by imaging will be important for the treatment of patients receiving anti-angiogenic therapies. Clinical imaging of angiogenesis should be designed to address the following aims:

1. *Selection of the optimal treatment*. The number of anti-angiogenic compounds entering clinical trials is rapidly increasing, and many additional compounds are at various stages of development each targeting a different point in the process. The efficacy of treatment could vary between tumours, and thus the choice of optimal treatment will require information on the biology and functional status of the tumour vasculature. Thus, characterisation of the angiogenic status of a tumour may allow the rational selection of specific treatments.
2. *Tailored dose optimisation based on the suppression of the specific activity*. Clinical trials of anti-angiogenic treatments have reported very low toxicity compared with chemotherapy; toxicity based selection of dose may therefore not be optimal for *in vivo* activity. Imaging may aid in dose selection if it were possible to show quantitative biological effects specified by a mechanism-based knowledge of drug action.
3. *Detection of early anti-angiogenic response*. The intrinsic redundancy of signalling mechanisms associated with angiogenesis will lead to partial or complete resistance of the tumour vessels to therapy. Interest in imaging techniques that can provide early indicators of effectiveness at a functional or molecular level has therefore increased. Tumour response to treatment can be detected by imaging techniques that are capable of monitoring changes in perfusion, blood volume or microvessel permeability.
4. *Analysis of the impact of treatment on tumour progression*. Monitoring the therapeutic effects of anti-angiogenic therapy is expected to be harder

to detect and quantify. This is because anti-angiogenic treatments may not result in substantial reductions in tumour volume and conventional size measurements of response may be insensitive or markedly delayed even when there is a significant antivascular effect. Imaging based approaches will also be valuable for monitoring chronic anti-angiogenic treatment as these therapies will be used for long-term stabilisation of cancer. As anti-angiogenic therapy is envisioned to require long-term treatment, non-invasive, cost-effective techniques would be highly desirable.

Specific molecular markers on newly formed vessels can be imaged by novel imaging techniques. Many of these markers have also been identified as potential targets of vascular-directed therapies. Specific examples of these kinds of imaging techniques include imaging of $\alpha\upsilon\beta3$ endothelial integrins by paramagnetic liposomes [20]. These paramagnetic liposomes can be designed to carry anti-angiogenic or cytotoxic drugs thus enabling both treatment and visualisation of angiogenic endothelium in tumours. Other approaches include targeting of angiogenesis-associated fibronectin isoforms using optical probes [21] and imaging labelled antibodies targeting tumour growth factor β receptor [22]. Tumour angiogenesis can also be analysed using intrinsic blood oxygenation level dependent (BOLD) contrast MRI for mapping mature and immature vessels and their differential sensitivity to perturbations in vascular endothelial growth factor (VEGF) expression [23]. This application of BOLD MRI is discussed in more detail below. A number of anti-angiogenic agents also cause endothelial and tumour cell apoptosis. Apoptosis is a physiological form of programmed cell death, which is critical for organ development, tissue homeostasis and for the removal of defective cells. Defects in the apoptotic pathway are important features of cancers. Markers of endothelial cell apoptosis, such as annexin V, may be adapted for radiolabelling thus enabling direct visualisation of sites where there is anti-angiogenic and antitumour drug action [24].

3. Clinical MRI assessment of microvessel function

MRI can be used experimentally and clinically to characterise tumour microvessel structure and function [25]. MRI techniques can be divided into non-enhanced and contrast media enhanced methods [26]. The latter can be further divided by the type of contrast medium utilised; (i) non-specific techniques that utilise small-molecular agents that distribute rapidly in the extracellular space (ECF agents), (ii) techniques that use large-molecular agents designed for prolonged intravascular retention (macromolecular contrast media, or blood pool agents) and (iii) methods that use agents intended to accumulate at sites of concentrated angiogenesis mediator molecules. ECF contrast agents are available commercially and the pathophysiological basis, validation, quantification and clinical applications of DCE-MRI will be discussed in detail. Macromolecular contrast media are in clinical development, but are not currently approved for human use. Molecular targeted contrast media are in preclinical development. MRI methods of evaluating microvessel function have the advantage of good spatial resolution often equal to that of corresponding morphological images. MRI techniques are minimally invasive and involve little patient risk. As such, they can be incorporated into routine patient studies. Limitations of MRI techniques are discussed below. Other imaging techniques that assess microvasculature have a number of drawbacks [27–29]. For example, ultrasound examinations are limited by poor depth of penetration and organs such as the brain and lungs remain inaccessible. Ultrasound is also highly operator-dependent. Radiation exposure considerations and the small volume of tissue that can be examined limits CT assessments. PET is limited by high cost and limited availability of equipment. Furthermore, the short lives of radioisotopes used require that a cyclotron and onsite radiochemistry be present.

4. Contrast agent kinetics using extracellular contrast agents

DCE-MRI is able to distinguish malignant from benign tissues by exploiting differences in contrast agent kinetics [30,31]. When a bolus of paramagnetic contrast agent passes through a capillary bed, it is initially confined in the intravascular space. Within this space, it produces magnetic field (Bo) inhomogenities that result in a decrease in the signal intensity of surrounding tissues. In most extracranial tissues and in some brain tumours, the contrast agent then passes into the extravascular-extracellular space (EES) at a rate determined by the permeability of the capillaries and their surface area. The early phase of contrast enhancement (often referred to as the 'first pass') includes the arrival of contrast medium and lasts many cardiac cycles. In this phase, the contrast medium gains access to the extracellular space via diffusion and causes shortening of tissue T1-relaxation times. The early signal increase observed on T1-weighted images arises from both the vascular and interstitial compartments. Contrast medium also begins to diffuse into tissue compartments further removed from the vasculature including areas of necrosis and fibrosis. Over a period typically lasting several minutes to half an hour, the contrast agent diffuses back into the vasculature from which it is excreted (usually by the kidneys). Contrast medium elimination

from very slow-exchange tissues such as fibrosis and necrosis occurs more slowly causing persistent delayed enhancement.

MR sequences can be designed to be sensitive to the vascular phase of contrast medium delivery (so-called T2* methods which reflect on tissue perfusion and blood volume). Similarly, sequences sensitive to the presence of contrast medium in the EES reflect on microvessel permeability and extracellular leakage space (so-called T1 methods). The analysis methods for evaluating these techniques have their foundations in basic physiology and pharmacology [32–34]. These two methods are compared in Table 1.

5. T2*-weighted imaging

Perfusion-weighted images can be obtained with 'bolus-tracking techniques' that monitor the passage of contrast material through a capillary bed [35,36]. The decrease in signal intensity of tissues can be observed with susceptibility-weighted T1- or T2*-weighted sequences, the latter providing greater sensitivity and contrast to perfusion effects. The degree of signal loss seen is dependent on the vascular concentration of the contrast agent and microvessel size [37] and volume. The signal to noise ratio (SNR) of such images can be improved by using higher doses of contrast medium (i.e. $\geqslant$0.2-mmol/kg body weight) [38]. High specification, echo-planar capable MRI systems capable of rapid image acquisition are required to adequately characterise these effects. However, such studies are possible on conventional MRI systems using standard gradient-echo sequences, but are limited to a few slices.

Tracer kinetic principles can be used to provide estimates of relative blood volume (rBV), relative blood flow (rBF) and mean transit time (MTT) derived from the first-pass of contrast agent through the microcirculation [39] (Fig. 1). These variables are related by the central volume theorem equation (BF = BV/MTT). BV measurements can obtained from the integral of time-susceptibility curves, but a number of conditions of the central volume theorem are not met. For example, injection time is not instantaneous (in general, not obtainable in biological tissues) and as the arterial input function is not typically measured, these parameters estimates are qualitative or 'relative'. Recently, quantification of these parameters has been undertaken by simultaneous monitoring of the concentration of contrast agent in a large neck or brain vessel [40] and quantified perfusion parameters in normal brain and low grade gliomas have been obtained [40,41].

Recirculation of contrast medium can impair the calculation of T2*-weighted parameter estimates. Other physiological effects that hinder accurate measurements include non-laminar flow, which arises from the presence of irregular calibre vessels, non-dichotomous branching and high vascular permeability, which leads to increased blood viscosity (from haemoconcentration). In addition, factors such as machine stability, patient motion and intrinsic patient variables particularly cardiac output and upstream stenoses can affect the computations. The quantification techniques described above also cannot readily be applied to areas of marked blood–brain barrier breakdown or to extracranial tumours with very leaky blood vessels. This is because the T1 enhancing effects of gadolinium chelates can counteract T2* signal lowering effects, resulting in

Table 1
Comparison of T2*- and T1-weighted dynamic contrast enhanced MR imaging techniques

	T2*W imaging	T1W imaging
Tissue signal intensity change	Darkening	Enhancement
Duration of effect and optimal data acquisition	Seconds/subsecond	Minutes/2–25 s
Magnitude of effect	Small	Larger
Optimal contrast medium dose	$\geqslant$0.2 mmol/kg	0.1–0.2 mmol/kg
Quantification method used	Relative more than absolute	Relative and absolute
Physiological property measured	Perfusion/blood volume	Transendothelial permeability, capillary surface area, lesion leakage space
Kinetic parameters derived	Blood volume and flow, transit time	Transfer and rate constants, leakage space
Pathological correlates	Tumour grade and microvessel vessel density	Microvessel density Vascular endothelial growth factor (VEGF)
Clinical MR applications	Lesion characterisation—breast, liver and brain	Lesion detection and characterisation
	Non-invasive brain tumour grading	Improving accuracy of tumour staging
	Directing brain tumour biopsy	Predicting response to treatment
	Determining brain tumour prognosis	Monitoring response to treatment
	Monitoring treatment, e.g. radiotherapy	Novel therapies including anti-angiogenesis drugs
	Novel therapies including anti-angiogenesis drugs	Detecting tumour relapse

MR, magnetic resonance.

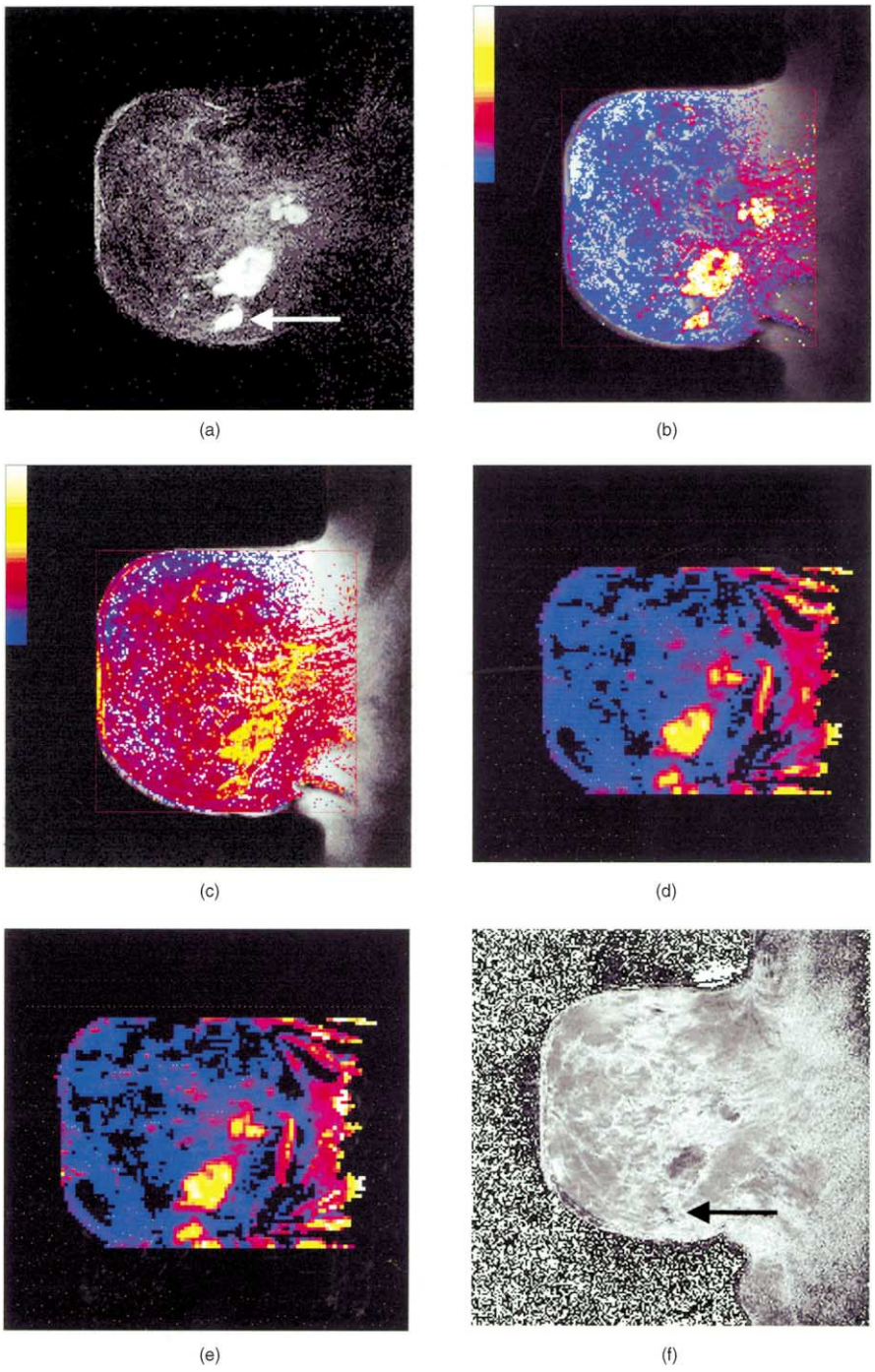

Fig. 1. Multifunctional MRI assessment of breast carcinoma. The following series of images were obtained from a 49-year-old woman with multifocal, invasive ductal breast cancer. All images were obtained in a time period acceptable to most patients (50 min). (a) Anatomical, sagittal post contrast enhanced, subtraction MR image of the breast shows multiple foci of irregular enhancement compatible with multifocal breast cancer. The arrow refers to a feature indicated in (f) below. Images (b) and (c) are obtained from a T1-weighted acquisition using 0.1 mmol/kg of contrast medium (Gadopentatate dimeglumine). (b) Transfer constant pixel map shows the permeability surface area product of the vasculature displayed as a pixel map on the anatomical image (maximum transfer constant displayed is 1.0 ml/ml/min). High transfer constant values compared with normal breast and heterogeneous distribution is typical of cancer. (c) Leakage space pixel map at the same slice position (maximum leakage space displayed 100%). Images (d) and (e) are obtained from a T2*-weighted acquisition using 0.2 mmol/kg of contrast medium. (d) Relative blood volume and (e) relative blood flow pixel maps have been obtained at a slightly lower spatial resolution, but at the same anatomical location. The tumour foci are noted to be markedly hypervascular. Note the good correspondence between perfusion parameters (d, blood volume and e, blood flow) and the permeability parameter maps (b, transfer constant). (f) Synthetic R2* maps calculated from a series of Blood Oxygenation Level Dependent (BOLD) images obtained at the same level. The BOLD images themselves are not shown. Lighter colours indicate poorer tissue oxygenation because of greater levels of deoxyhaemoglobin. The largest lesion is better oxygenated than normal tissues. A disparity between tissue oxygenation (greater deoxyhaemoglobin) and blood flow (high flow) is seen in the lowest lesion on its posterior aspect indicated by the arrows on (a) and (f).

falsely low blood volume values in very leaky vessels. Quantitative imaging is thus most reliably used for normal brain and non-enhancing brain lesions (e.g. low-grade gliomas) because the contrast medium is retained within the intravascular space. One solution to overcoming these problems is to use non-gadolinium susceptibility contrast agents based on the element dysprosium, which has a strong T2* effect, but a weak T1 effect [42,43].

The signal loss observed with T2*-weighted sequences have been used qualitatively in clinical studies to characterise liver, breast and brain tumours [44–46]. Relative cerebral blood volume (rCBV) mapping can be used to detect areas of increased vascularity in brain gliomas [47,48]. Areas of high tumour rCBV appear to correlate with tumour grade and vascularity, but not with cellular atypia, endothelial proliferation, necrosis or cellularity [47]. In low-grade gliomas, homogeneous low rCBV is found whereas high-grade tumours display both low and high rCBV components [49]. Cerebral blood volume maps can therefore be used to direct stereotactic biopsy to areas where high tumour grade may be found [50,51]. Other potential uses of T2*W imaging in patients with brain tumours include distinguishing radiation necrosis from recurrent disease, determining prognosis and monitoring response to radiotherapy [41]. Recently, T2*-weighted MRI has been used to monitor the treatment effects of thalidomide administered with carboplatin in patients with recurrent malignant gliomas [52]. This preliminary report showed that changes on T2*-weighted images correlated more closely with the clinical status of patients than conventional contrast enhanced images, possibly because enhancement on T1-weighted images is not specific for active tumour.

6. T1-weighted imaging

Extracellular contrast media readily diffuse from the blood into the EES of tissues at a rate determined by the permeability of the capillaries and their surface area. Shortening of T1 relaxation time caused by contrast medium is the mechanism of tissue enhancement. Most DCE-MRI studies employ gradient-echo sequences to monitor the tissue enhancing effects of contrast media. This is because gradient-echo sequences have good contrast medium sensitivity, high signal-to-noise ratio and data acquisition can be performed rapidly. The degree of signal enhancement seen on T1-weighted images is dependent on a number of physiological and physical factors. These include tissue perfusion, capillary permeability to contrast agent, volume of the extracellular leakage space, native T1-relaxation time of the tissue, contrast agent dose, imaging sequence used and parameters utilised and on machine scaling factors [53,54].

Signal enhancement seen on a dynamic acquisition of T1-weighted images can be assessed in two ways: by the analysis of signal intensity changes (semi-quantitative) and/or by quantifying contrast agent concentration change using pharmacokinetic modelling techniques [55]. Semi-quantitative parameters describe tissue signal intensity enhancement using of a number of descriptors. These parameters include onset time (time from injection to the arrival of contrast medium in the tissue), initial and mean gradient of the upslope of enhancement curves, maximum signal intensity and washout gradient. As the rate of enhancement is important for improving the specificity of examinations, parameters that include an additional time element are also used (e.g. maximum intensity time ratio (MITR) [56] and maximum focal enhancement at 1 min [57,58]). Semi-quantitative parameters have the advantage of being relatively straightforward to calculate, but have a number of limitations. These include the fact that they do not accurately reflect tissue contrast medium concentration or the vascular endpoint of interest (tissue perfusion, blood volume and capillary permeability). Semi-quantitative estimates are also subject to the variabilities of scanner manufacture and examination settings (including gain and scaling factors). These limitations can and do make between-patients and system comparisons difficult.

Quantitative techniques use pharmacokinetic modelling techniques that are usually applied to tissue contrast agent concentration changes. Signal intensity changes observed during dynamic acquisition are used to estimate contrast agent concentration *in vivo* [55,59,60]. Concentration–time curves are then mathematically fitted using one of a number of recognised pharmacokinetic models [61]. Examples of modelling parameters include the volume transfer constant of the contrast agent (K^{trans}—formally called permeability-surface area product per unit volume of tissue), leakage space as a percentage of unit volume of tissue (v_e) and the rate constant (k_{ep} also called K_{21}) (Fig. 1). These parameters are related mathematically ($k_{ep} = K^{trans}/v_e$) and recently have been reconciled with others that appear in the literature [62]. It is important to note that in tissues with highly permeable vessels, the rate at which the contrast medium enters the EES is limited by perfusion and in this situation the transfer constant (K^{trans}) is equivalent to the plasma flow per unit volume of tissue [63]. In tissues such as the brain where an intact blood–brain barrier limits the rate at which the contrast medium enters the EES, K^{trans} is equivalent to the permeability surface area product. In malignant tumours, vessels in general are more permeable than normal tissues, but are heterogeneously distributed and therefore K^{trans} reflects a combination of permeability surface area product and perfusion. Quantitative parameters are more complicated to derive compared with those derived semi-quantitatively. The model chosen may not

fit the data obtained, and each model makes a number of assumptions that may not be valid for every tissue or tumour type [61,62]. None the less, if contrast agent concentration can be measured accurately and the type, volume and method of administration are consistent, then it may possible to directly compare pharmacokinetic parameters acquired serially in a given patient and in different patients imaged at the same or different scanning sites [63].

Many studies have attempted to correlated tissue MR enhancement with immuno-histochemical microvessel density (MVD) measurements [26]. A number of studies have shown broad correlation between MR enhancement and MVD [64–67], whereas others have found no correlation [68,69]. Experience shows that factors other than microvessel density must be important in determining the degree of tissue enhancement. For example, in the brain, retina and testis, high vascular density and capillary permeability estimates do not correlate because of an intact capillary–interstitial space barrier. Recently, VEGF a potent vascular permeability and angiogenic factor has been implicated as an additional explanatory factor that determines MR signal enhancement. Knopp and colleagues [70] reported that vascular permeability to contrast media closely correlated with tissue VEGF expression in breast tumours. The importance of the role of VEGF in determining microvascular permeability is supported by the spatial association of hyperpermeable capillaries and VEGF expression on histological specimens [71,72]. A correlation between serum VEGF levels and rectal tumour K^{trans} values has recently been reported [73]. Furthermore, the observation that MR kinetic measurements can detect suppression of vascular permeability after anti-VEGF antibody [74] and after the administration of inhibitors of VEGF signalling [75] lends weight to the important role played by VEGF in determining MR enhancement. Other characteristics that have been correlated with enhancement patterns include the degree of stromal cellularity and fibrosis [76,77], tissue oxygenation [69] and tumour grade [78].

Analysis of enhancement seen on dynamic T1-weighted is a valuable diagnostic tool in a number of clinical situations. The most established role is in lesion characterisation where it has found a role in distinguishing benign from malignant breast and musculoskeletal lesions [57,79]. Dynamic T1-weighted MRI studies have also been found to be of value in staging gynaecological malignancies, bladder and prostate cancers [80,81]. Most recently, enhancement parameters have been shown to predict survival in patients with cervical cancers; that is, tumours with fast initial rate of enhancement or vascular permeability were more likely to have a poorer prognosis [82] despite having a higher radiotherapy response rate [83]. DCE-MRI studies have also been found to be of value in detecting tumour relapse within treated tissues of the breast and pelvis [84–88].

DCE-MRI is also able to predict response or monitor the effects of a variety of treatments. These include neoadjuvant chemotherapy in bladder and breast cancers and bone sarcomas [89–92]. In breast cancer, for example, it has recently been shown that a decrease in transendothelial permeability accompanies tumour shrinkage and that an early (1–2 cycles of chemotherapy) increase or no change in permeability can predict non-responsiveness [93]. Other treatments that can be monitored include radiotherapy (Fig. 2) of rectal and cervical cancers [73,94,95], androgen deprivation in prostate cancer [96] and vascular embolisation of uterine fibroids [97]. All these studies show that successful treatment results in a decrease in the rate of enhancement and that poor response results in persistent abnormal enhancement however judged (semi-quantitatively or quantitatively). A number of studies have recently reported on the use of T1-weighted MRI for monitoring the effects of anti-angiogenic/antivascular treatments [75,98,99].

7. Promising new MRI approaches

7.1. Macro-molecular MR assays of microvascular function

MRI assays of tumour angiogenesis using macromolecular contrast agents (MMCM) should be feasible soon. MMCM-enhanced MRI parameters of tumour microvessel characteristics include vascular permeability (kPS) and the fractional plasma volume (fPV) [100]. Physiologists have observed that the microvessels of cancer are hyperpermeable to macromolecules, a feature largely absent in normal vessels [101,102]. Hyperpermeability to macromolecules is considered important, even essential, to angiogenesis because it allows plasma proteins to seep into the tumour interstitium forming the matrix for the subsequent in-growth of new capillaries. Data analyses in animal models have shown good correlation between MRI-derived assays of tumour kPS and fPV with histological microvessel density (MVD) [103,104]. Preclinical studies have also demonstrated that MMCM-enhanced MRI could identify and measure the effect of an anti-VEGF antibody on tumour vascular permeability [74]. This study showed that MMCM estimates of vascular permeability were highly sensitive to angiogenesis modulation as early as 24 h after a single dose of anti-VEGF antibody. The fractional plasma volume did not change significantly suggesting that this characteristic, dependent on vessel morphology (MVD and surface area) is less sensitive than permeability to inhibition of VEGF. Macromolecular MRI contrast media for use in clinical studies

of anti-angiogenesis/antivascular drugs has not been approved.

7.2. Imaging vascular function using haemoglobin as a contrast agent

Analysis of vascular function can be accomplished by using deoxyhaemoglobin as an intrinsic, paramagnetic contrast agent (blood oxygenation level dependent or BOLD contrast) [105]. Gradient-echo T_2* weighted images that are sensitive to changes in blood volume, blood flow and blood oxygenation are used. BOLD contrast can be used for mapping changes in blood volume fraction, and vascular functionality associated with angiogenesis [106,107]. Multi-gradient echo techniques allow the calculation of relaxation (R_2*) maps that are exclusively sensitive to tissue oxygenation (Fig. 1f). Vascular function can be evaluated by analysis of BOLD contrast changes in response to hyperoxia and hypercapnia [106,108]. Clinical application of this

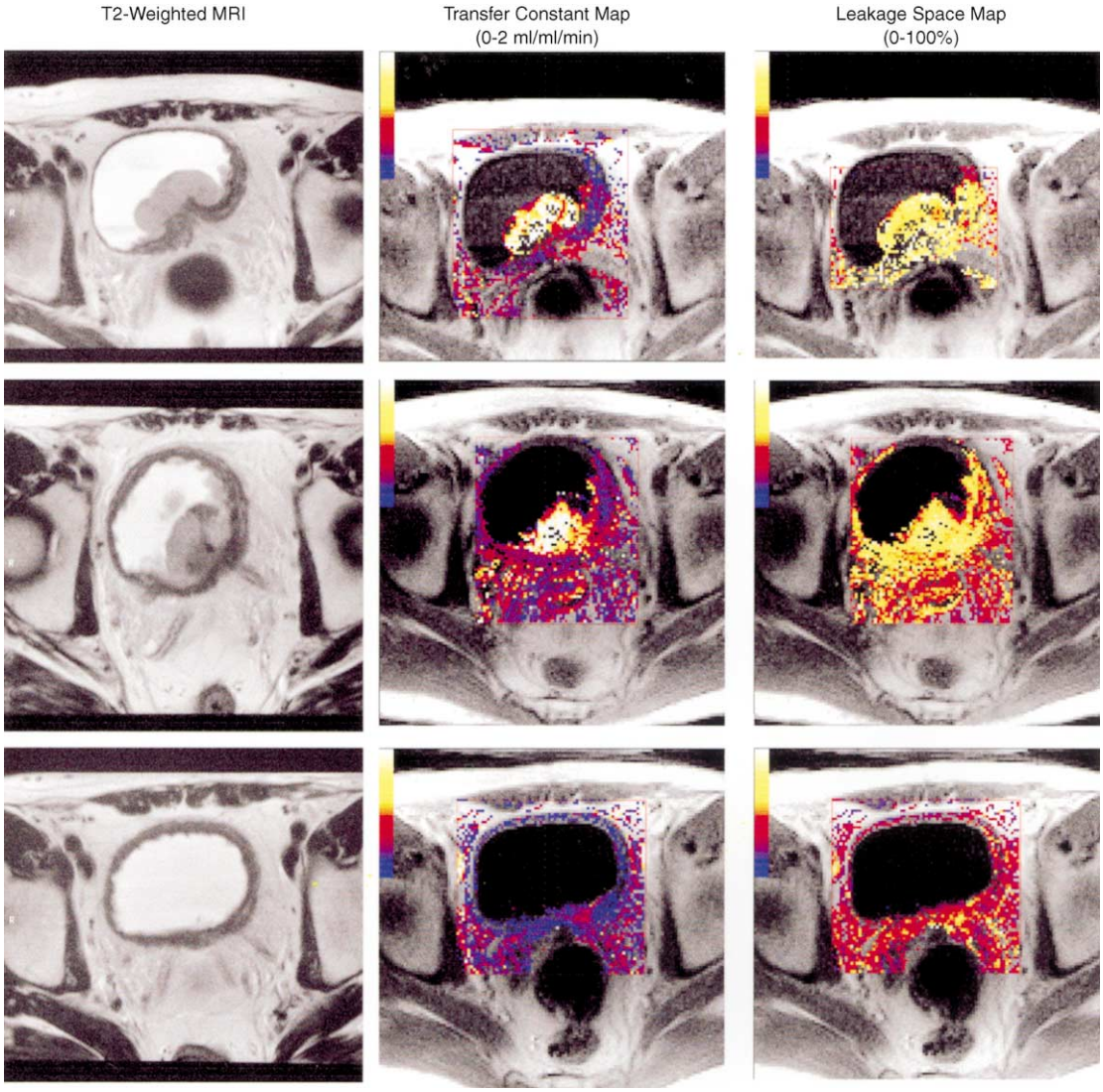

Fig. 2. Monitoring radiotherapy response of bladder cancer with DCE-MRI. *Columns*: anatomical T2-weighted MR images of a transitional cell bladder carcinoma, transfer constant maps (colour display range 0–2 ml/ml/min) and leakage space maps (colour display range 0–100%) in a patient being treated with radiotherapy. *Top row*: Baseline images show that the bladder wall is markedly thickened, but has a low transfer constant suggesting that the thickening is not due to tumour infiltration. The stalk of the tumour has intermediate transfer constant values. A number of pixels within the tumour show no colour (modelling failures). Median tumour transfer constant value 1.39 ml/ml/min, leakage space values 70%, and rate constant value 1.98 ml/ml/min. *Middle row:* 30 days after starting radiotherapy (44 gray), the tumour has changed in shape, but continues to show high transfer constant values. The wall and fatty tissues around the bladder now show increased transfer constant (increased capillary permeability) and leakage space. These features are consistent with vascular damaging effects of radiotherapy. Median tumour transfer constant value 0.64 ml/ml/min, leakage space values 59%, and rate constant value 1.18 ml/ml/min. *Bottom row:* 30 days after the completion of treatment (total dose administered 60 gray), the tumour mass has almost completely regressed, but the bladder wall continues to be thickened. Marked reductions in transfer constant and leakage space are now observed. Median tumour transfer constant value 0.29 ml/ml/min, leakage space values 45%, rate constant value 0.66 ml/ml/min. (Reprinted by kind permission of W.B. Saunders and *Clinical Radiology* [16].).

technique has revealed high signal enhancements in response to carbogen (5% CO_2: 95%O_2) inhalation in human tumours [109]. Taylor and colleagues have also reported that human studies are technical challenging [109]. The primary advantage of BOLD techniques is that there is no need to administer contrast material. Measurements can be repeated as needed with almost no limitation. BOLD contrast is not sensitive to fluctuation in permeability. A major reservation for intrinsic contrast imaging is the low contrast to noise ratio in the images obtained.

8. Challenges for functional MRI techniques

From the above discussion, it is clear that a variety of MRI techniques can evaluate microvascular structure and function. This variety can make it difficult to make meaningful comparisons between different tissue types and to compare data obtained from different imaging centres. The clinical imaging community needs to agree on a limited number of examination and analysis protocols in order to enable techniques to be validated and used in clinical trials. Another issue that needs to be addressed is that of data collection in body parts where there is a large degree of physiological movement such as the lungs and liver. Some techniques such as PET are unable to demonstrate heterogeneity within tumours at high spatial resolution and for such techniques, physiological motion does not appear to be a problem. However, for CT and MRI, the presence of motion can invalidate functional vascular parameter estimates. Quantification techniques aim to minimise errors that can result from the use of different equipment and imaging protocols. Quantification techniques also enable the derivation of kinetic parameters that are based on some understanding of physiological processes and so can provide insights into tumour biology. Quantification techniques are therefore preferred when evaluating angiogenic interventions. Quantification techniques often rely on the application of a mathematical model to the data acquired. Experience shows that such models may not fit the data observed. The causes of such modelling failures are complex and often not well understood. We do not have models that fit all data and more sophisticated models that provide insights into tissue compartment behaviour are needed.

Measurement error is the variation between measurements of the same quantity on the same individual. An estimate of measurement error enables us to decide whether a change in observation represents a real change. Data addressing the precision and measurement variability of different imaging techniques is urgently needed and should be an integral part of any new prospective study that evaluates the functional response to therapy. Factors that determine measurement error for a given technique also need to be defined. Any imaging assay of tumour microvascular characteristics must be rigorously validated against accepted surrogates of angiogenesis. Unfortunately, no single imaging assay or surrogate may be adequate to reflect the whole spectrum of events involved in angiogenesis. Commonly used and appropriate surrogates include histological microvascular density (MVD) as counted on factor VIII or CD34-stained tumour specimens and vascular maturation index (VMI) [26]. Also, quantitative measures of VEGF or other known mediators of angiogenesis, in the tumour tissue itself, or in the plasma, can be compared to the imaging assay results. Similarly, the imaging assays need to be tested against each other in order to determine their relative utility. Analysis and presentation of imaging data needs to take into account the heterogeneity of tumour vascular characteristics. Pixel mapping techniques (Figs. 1 and 2) with histogram analysis are methods by which such heterogeneity can be displayed and quantified.

9. Conclusions

Functional MRI techniques have the potential to act as new tumour response variables. Some parameters have already been investigated for their potential as tumour response parameters, but there have been few large correlative studies. Anatomical and multifunctional response assessment studies are difficult to perform because of costs, availability of equipment and expertise, lack of robust image registration procedures (particularly in extracranial applications) and due to time constraints that are acceptable to patients and institutional ethics committees. This is particularly the case where such evaluations have to be repeated to determine the optimal timing for response of individual parameters. The importance of being able to perform combined multifunctional and morphological examinations cannot be overemphasised; they will enable coregistration of anatomical and functional data and so allow an appreciation of tumour heterogeneity, and will enable correlation between different and diverse functional parameters. Furthermore, they should allow longitudinal outcome studies to be performed, which will lead to an improved understanding of aspects of tumour biology and treatment response, which in turn may improve patient staging, treatment stratification and determination of prognosis. These techniques will also have a central role in the evaluation of novel therapies, for example, anti-angiogenesis drugs, gene therapy and antibody treatments. Given the lead-time between the development of a therapeutic approach of a drug in the laboratory and its evaluation in the clinic, clinicians and radiologists would do well to fully

evaluate currently available and new imaging technologies as potential response parameters.

Acknowledgements

I gratefully acknowledge the advice of Professor J. E. Husband, Professor M. O. Leach. The Cancer Research Campaign (CRC) generously supports research within the MRI Unit at the Royal Marsden Hospital and Institute of Cancer Research, London, where some of the illustrated work was obtained.

References

1. Miller A, *et al*. Reporting results of cancer treatment. *Cancer* 1981, **47**, 207–214.
2. WHO. *WHO Handbook for Reporting Results of Cancer Treatment*. *Offset Publication No. 48*. Geneva, Switzerland, World Health Organization, 1979.
3. Hawthorn J. *A Practical Guide to EORTC Studies*. Brussels, European Organisation for the Research and Treatment of Cancer (EORTC), 1994.
4. Therasse P, *et al*. New guidelines to evaluate the response to treatment in solid tumors. European Organization for Research and Treatment of Cancer, National Cancer Institute of the United States, National Cancer Institute of Canada. *J Natl Cancer Inst* 2000, **92**, 205–216.
5. Thiesse P, *et al*. Response rate accuracy in oncology trials: reasons for interobserver variability. Groupe Francais d'Immunotherapie of the Federation Nationale des Centres de Lutte Contre le Cancer. *J Clin Oncol* 1997, **15**, 3507–3514.
6. Smith TA. FDG uptake, tumour characteristics and response to therapy: a review. *Nucl Med Commun* 1998, **19**, 97–105.
7. Hoekstra OS, *et al*. Early treatment response in malignant lymphoma, as determined by planar fluorine-18-fluorodeoxyglucose scintigraphy. *J Nucl Med* 1993, **34**, 1706–1710.
8. Husband JE, Hawkes DJ, Peckham MJ. CT estimations of mean attenuation values and volume in testicular tumours: a comparison with surgical and histologic findings. *Radiology* 1982, **144**, 553–558.
9. Weissleder R. Molecular imaging exploring the next frontier. *Radiology* 1999, **212**, 609–614.
10. Folkman J. The role of angiogenesis in tumour growth. *Semin Cancer Biol* 1992, **3**, 65–71.
11. Folkman J. Angiogenesis in cancer, vascular, rheumatoid and other disease. *Nat Med* 1995, **1**, 27–31.
12. Brown JM, Giaccia AJ. The unique physiology of solid tumors: opportunities (and problems) for cancer therapy. *Cancer Res* 1998, **58**, 1408–1416.
13. Tomida A, Tsuruo T. Drug resistance mediated by cellular stress response to the microenvironment of solid tumors. *Anticancer Drug Des* 1999, **14**, 169–177.
14. Wells P, Harte RJA, Price P. Positron emission tomography: a new investigational area for cancer research. *Clin Oncol* 1996, **8**, 7–14.
15. Robinson SP, Barton SJ, McSheehy PM, Griffiths JR. Nuclear magnetic resonance spectroscopy of cancer. *Br J Radiol* 1997, **70**, S60–S69.
16. Padhani AR, Husband JE. Dynamic contrast-enhanced MRI studies in oncology with an emphasis on quantification, validation and human studies. *Clin Radiol* 2001, **56**, 607–620.
17. Chenevert TL, Stegman LD, Taylor JM, *et al*. Diffusion magnetic resonance imaging: an early surrogate marker of therapeutic efficacy in brain tumours. *J Natl Cancer Inst* 2000, **92**, 2029–2036.
18. Koh WJ, *et al*. Imaging of hypoxia in human tumors with [F-18] fluoromisonidazole. *Int J Radiat Oncol Biol Phys* 1992, **22**, 199–212.
19. Weissleder R, Mahmood U. Molecular imaging. *Radiology* 2001, **219**, 316–333.
20. Sipkins DA, Cheresh DA, Kazemi MR, Nevin LM, Bednarski MD, Li KC. Detection of tumour angiogenesis in vivo by alphaVbeta3-targeted magnetic resonance imaging. *Nat Med* 1998, **4**, 623–626.
21. Nevi D, Carnemolla B, Nissim A, *et al*. Targeting by affinity-matured recombinant antibody fragments of an angiogenesis associated fibronectin isoform. *Nat Biotechnol* 1997, **15**, 1271–1275.
22. Bredow S, Lewin M, Hoffmann B, Marecos E, Weissleder R. Imaging of tumour neovasculature by targeting the TGF-beta binding receptor endoglin. *Eur J Cancer* 2000, **36**, 675–681.
23. Abramovitch R, Dafni H, Smouha E, *et al*. In vivo prediction of vascular susceptibility to vascular endothelial growth factor withdrawal: magnetic resonance imaging of C6 rat glioma in nude mice. *Cancer Res* 1999, **59**, 5012–5016.
24. Blankenberg FG, Katsikis PD, Tait JF, *et al*. In vivo detection and imaging of phosphatidylserine expression during programmed cell death. *Proc Natl Acad Sci USA* 1998, **95**, 6349–6354.
25. Neeman M, Provenzale JM, Dewhirst MW. Magnetic resonance imaging applications in the evaluation of tumor angiogenesis. *Semin Radiat Oncol* 2001, **1**, 70–82.
26. Brasch RC, Li KC, Husband JE, *et al*. In vivo monitoring of tumor angiogenesis with MR imaging. *Acad Radiol* 2000, **7**, 812–823.
27. Blankenberg FG, Eckelman WC, Strauss HW, *et al*. Role of radionuclide imaging in trials of antiangiogenic therapy. *Acad Radiol* 2000, **7**, 851–867.
28. Miles KA, Charnsangavej C, Lee FT, Fishman EK, Horton K, Lee TY. Application of CT in the investigation of angiogenesis in oncology. *Acad Radiol* 2000, **7**, 840–850.
29. Ferrara KW, Merritt CR, Burns PN, Foster FS, Mattrey RF, Wickline SA. Evaluation of tumor angiogenesis with US: imaging, Doppler, and contrast agents. *Acad Radiol* 2000, **7**, 824–839.
30. Yuh WT. An exciting and challenging role for the advanced contrast MR imaging. *J Magn Reson Imaging* 1999, **10**, 221–222.
31. Taylor JS, Tofts PS, Port R, *et al*. MR imaging of tumor microcirculation: promise for the new millennium. *J Magn Reson Imaging* 1999, **10**, 903–907.
32. Zierler KL. Theory of use of indicators to measure blood flow and extracellular volume and calculation of trans capillary movement of tracers. *Circulation Res* 1963, **12**, 464–471.
33. Crone C. The permeability of capillaries in various organs as determined by the use of indicator diffusion' method. *Acta Physiol Scand* 1963, **58**, 292–305.
34. Kety SS. The theory and applications of the exchange of inert gas at the lungs and tissues. *Pharmacol Rev* 1951, **3**, 1–41.
35. Rosen BR, Belliveau JW, Aronen HJ, *et al*. Susceptibility contrast imaging of cerebral blood volume: human experience. *Magn Reson Med* 1991, **22**, 293–299.
36. Edelman RR, Mattle HP, Atkinson DJ, *et al*. Cerebral blood flow: assessment with dynamic contrast-enhanced T2*-weighted MR imaging at 1.5 T. *Radiology* 1990, **176**, 211–220.
37. Dennie J, Mandeville JB, Boxerman JL, Packard SD, Rosen BR, Weisskoff RM. NMR imaging of changes in vascular morphology due to tumor angiogenesis. *Magn Reson Med* 1998, **40**, 793–799.

38. Bruening R, Berchtenbreiter C, Holzknecht N, *et al*. Effects of three different doses of a bolus injection of gadodiamide: assessment of regional cerebral blood volume maps in a blinded reader study. *Am J Neuroradiol* 2000, **21**, 1603–1610.
39. Sorensen AG, Tievsky AL, Ostergaard L, Weisskoff RM, Rosen BR. Contrast agents in functional MR imaging. *J Magn Reson Imaging* 1997, **7**, 47–55.
40. Rempp KA, Brix G, Wenz F, Becker CR, Guckel F, Lorenz WJ. Quantification of regional cerebral blood flow and volume with dynamic susceptibility contrast-enhanced MR imaging. *Radiology* 1994, **193**, 637–641.
41. Wenz F, Rempp K, Hess T, *et al*. Effect of radiation on blood volume in low-grade astrocytomas and normal brain tissue: quantification with dynamic susceptibility contrast MR imaging. *Am J Roentgenol* 1996, **166**, 187–193.
42. Moseley ME, Vexler Z, Asgari HS, *et al*. Comparison of Gd- and Dy-chelates for T2 contrast-enhanced imaging. *Magn Reson Med* 1991, **22**, 259–264.
43. Lev MH, Kulke SF, Sorensen AG, *et al*. Contrast-to-noise ratio in functional MRI of relative cerebral blood volume with sprodiamide injection. *J Magn Reson Imaging* 1997, **7**, 523–527.
44. Ichikawa T, Haradome H, Hachiya J, Nitatori T, Araki T. Characterisation of hepatic lesions by perfusion-weighted MR imaging with an echoplanar sequence. *Am J Roentgenol* 1998, **170**, 1029–1034.
45. Kuhl CK, Bieling H, Gieseke J, *et al*. Breast neoplasms: T2* susceptibility-contrast, first-pass perfusion MR imaging. *Radiology* 1997, **202**, 87–95.
46. Kvistad KA, Lundgren S, Fjosne HE, Smenes E, Smethurst HB, Haraldseth O. Differentiating benign and malignant breast lesions with T2*-weighted first pass perfusion imaging. *Acta Radiol* 1999, **40**, 45–51.
47. Aronen HJ, Gazit IE, Louis DN, *et al*. Cerebral blood volume maps of gliomas: comparison with tumour grade and histologic findings. *Radiology* 1994, **191**, 41–51.
48. Sugahara T, Korogi Y, Kochi M, *et al*. Correlation of MR imaging-determined cerebral blood volume maps with histologic and angiographic determination of vascularity of gliomas. *Am J Roentgenol* 1998, **171**, 1479–1486.
49. Aronen HJ, Glass J, Pardo FS, *et al*. Echo-planar MR cerebral blood volume mapping of gliomas. Clinical utility. *Acta Radiol* 1995, **36**, 520–528.
50. Knopp EA, Cha S, Johnson G, *et al*. Glial neoplasms: dynamic contrast-enhanced T2*-weighted MR imaging. *Radiology* 1999, **211**, 791–798.
51. Bagley LJ, Grossman RI, Judy KD, *et al*. Gliomas: correlation of magnetic susceptibility artifact with histologic grade. *Radiology* 1997, **202**, 511–516.
52. Cha S, Knopp EA, Johnson G, *et al*. Dynamic contrast-enhanced T2-weighted MR imaging of recurrent malignant gliomas treated with thalidomide and carbolatin. *Am J Neuroradiol* 2000, **21**, 881–890.
53. Roberts TP. Physiologic measurements by contrast-enhanced MR imaging: expectations and limitations. *J Magn Reson Imaging* 1997, **7**, 82–90.
54. Evelhoch JL. Key factors in the acquisition of contrast kinetic data for oncology. *J Magn Reson Imaging* 1999, **10**, 254–259.
55. Parker GJM, Suckling J, Tanner SF, *et al*. Probing tumor microvessel density by measurement, analysis and display of contrast agent uptake kinetics. *J Magn Reson Imaging* 1997, **7**, 564–574.
56. Flickinger FW, Allison JD, Sherry RM, Wright JC. Differentiation of benign from malignant breast masses by time-intensity evaluation of contrast enhanced MRI. *Magn Reson Imaging* 1993, **11**, 617–620.
57. Kaiser WA, Zeitler E. MR imaging of the breast: fast imaging sequences with and without Gd-DTPA—preliminary observations. *Radiology* 1989, **170**, 681–686.
58. Gribbestad IS, Nilsen G, Fjosne HE, Kvinnsland S, Haugen OA, Rinck PA. Comparative signal intensity measurements in dynamic gadolinium-enhanced MR mammography. *J Magn Reson Imaging* 1994, **4**, 477–480.
59. Hoffmann U, Brix G, Knopp MV, Hess T, Lorenz WJ. Pharmacokinetic mapping of the breast: a new method for dynamic MR mammography. *Magn Reson Med* 1995, **33**, 506–514.
60. Parker GM, Baustert I, Tanner SF, Leach MO. Improving image quality and T1 measurements using saturation recovery TurboFLASH with approximate K-space normalisation filter. *Magn Reson Imaging* 2000, **18**, 157–167.
61. Tofts PS. Modelling tracer kinetics in dynamic Gd-DTPA MR imaging. *J Magn Reson Imaging* 1997, **7**, 91–101.
62. Tofts PS, Brix G, Buckley DL, *et al*. Estimating kinetic parameters from dynamic contrast-enhanced T(1)-weighted MRI of a diffusable tracer: standardized quantities and symbols. *J Magn Reson Imaging* 1999, **10**, 223–232.
63. Tofts PS, Berkowitz B, Schnall MD. Quantitative analysis of dynamic Gd-DTPA enhancement in breast tumors using a permeability model. *Magn Reson Med* 1995, **33**, 564–568.
64. Stomper PC, Winston JS, Herman S, Klippenstein DL, Arredondo MA, Blumenson LE. Angiogenesis and dynamic MR imaging gadolinium enhancement of malignant and benign breast lesions. *Breast Cancer Res Treat* 1997, **45**, 39–46.
65. Hawighorst H, Knapstein PG, Weikel W, *et al*. Angiogenesis of uterine cervical carcinoma: characterization by pharmacokinetic magnetic resonance parameters and histological microvessel density with correlation to lymphatic involvement. *Cancer Res* 1997, **57**, 4777–4786.
66. Tynninen O, Aronen HJ, Ruhala M, *et al*. MRI enhancement and microvascular density in gliomas. Correlation with tumor cell proliferation. *Invest Radiol* 1999, **34**, 427–434.
67. Buckley DL, Drew PJ, Mussurakis S, Monson JR, Horsman A. Microvessel density of invasive breast cancer assessed by dynamic Gd-DTPA enhanced MRI. *J Magn Reson Imaging* 1997, **7**, 461–464.
68. Hulka CA, Edmister WB, Smith BL, *et al*. Dynamic echo-planar imaging of the breast: experience in diagnosing breast carcinoma and correlation with tumor angiogenesis. *Radiology* 1997, **205**, 837–842.
69. Cooper RA, Carrington BM, Loncaster JA, *et al*. Tumor oxygenation levels correlate with dynamic contrast-enhanced magnetic resonance imaging parameters in carcinoma of the cervix. *Rad Oncol* 2000, **57**, 53–59.
70. Knopp MV, Weiss E, Sinn HP, *et al*. Pathophysiologic basis of contrast enhancement in breast tumours. *J Magn Reson Imaging* 1999, **10**, 260–266.
71. Furman-Haran E, Margalit R, Grobgeld D, Degani H. Dynamic contrast-enhanced magnetic resonance imaging reveals stress-induced angiogenesis in MCF7 human breast tumors. *Proc Natl Acad Sci USA* 1996, **93**, 6247–6251.
72. Bhujwalla ZM, Artemov D, Natarajan K, Ackerstaff E, Solaiyappam M. Vascular differences detected by MRI for metastatic versus nonmetastatic breast and prostate cancer xenografts. *Neoplasia* 2001, **3**, 143–153.
73. George ML, Dzik-Jurasz ASK, Padhani AR, *et al*. Non-invasive methods of assessing angiogenesis and their value in predicting response to treatment in colorectal cancer. *Br. J. Surg* [in press].
74. Pham CD, Roberts TP, van Bruggen N, *et al*. Magnetic resonance imaging detects suppression of tumor vascular permeability after administration of antibody to vascular endothelial growth factor. *Cancer Invest* 1998, **16**, 225–230.
75. Thomas A, Morgan B, Drevs J, *et al*. Pharmacodynamic results using dynamic contrast enhanced magnetic resonance imaging, of 2 phase 1 studies of the VEGF inhibitor PTK787/ZK 222584 in patients with liver metastases from colorectal cancer. *Proc Am Soc Clin Oncol* 2001, **20**, A279.

76. Matsubayashi R, Matsuo Y, Edakuni G, Satoh T, Tokunaga O, Kudo S. Breast masses with peripheral rim enhancement on dymanic contrast-enhanced MR images: correlation of MR findings with histologic features and expression of growth factors. *Radiology* 2000, **217**, 841–848.
77. Yamashita Y, Baba T, Baba Y, *et al*. Dymanic contrast-enhanced MR imaging of uterine cervical cancer: pharmacokinetic analysis with histopathologis correlation and its importance in predicting the outcome of radiation therapy. *Radiology* 2000, **216**, 803–809.
78. Roberts HC, Roberts TP, Brasch RC, Dillon WP. Quantitative measurement of microvascular permeability in human brain tumours achieved using dynamic contrast-enhanced MR imaging: correlation with histologic grade. *Am J Neuroradiol* 2000, **21**, 891–899.
79. Verstraete KL, De Deene Y, Roels H, Dierick A, Uyttendaele D, Kunnen M. Benign and malignant musculoskeletal lesions: dynamic contrast-enhanced MR imaging-parametric "first-pass" images depict tissue vascularization and perfusion. *Radiology* 1994, **192**, 835–843.
80. Liu PF, Krestin GP, Huch RA, *et al*. MRI of the uterus, uterine cervix, and vagina: diagnostic performance of dynamic contrast-enhanced fast multiplanar gradient-echo imaging in comparison with fast spin-echo T2-weighted pulse imaging. *Eur Radiol* 1998, **8**, 433–1440.
81. Barentsz JO, Jager GJ, van Vierzen PB, *et al*. Staging urinary bladder cancer after transurethral biopsy: value of fast dynamic contrast-enhanced MR imaging. *Radiology* 1996, **201**, 185–193.
82. Hawighorst H, Weikel W, Knapstein PG, *et al*. Angiogenic activity of cervical carcinoma: assessment by functional magnetic resonance imaging-based parameters and a histomorphological approach in correlation with disease outcome. *Clin Cancer Res* 1998, **4**, 2305–2312.
83. Mayr NA, Yuh WT, Magnotta VA, *et al*. Tumor perfusion studies using fast magnetic resonance imaging technique in advanced cervical cancer: a new noninvasive predictive assay. *Int J Radiat Oncol Biol Phys* 1996, **36**, 623–633.
84. Dao TH, Rahmouni A, Campana F, Laurent M, Asselain B, Fourquet A. Tumour recurrence versus fibrosis in the irradiated breast: differentiation with dynamic gadolinium-enhanced MR imaging. *Radiology* 1993, **187**, 751–755.
85. Heywang-Kobrunner SH, Schlegel A, Beck R, *et al*. Contrast-enhanced MRI of the breast after limited surgery and radiation therapy. *J Comput Assist Tomogr* 1993, **17**, 891–900.
86. Kinkel K, Tardivon AA, Soyer P, *et al*. Dynamic contrast-enhanced subtraction versus T2-weighted spin-echo MR imaging in the follow-up of colorectal neoplasm. A prospective study of 41 patients. *Radiology* 1996, **200**, 453–458.
87. Hawnaur JM, Zhu XP, Hutchinson CE. Quantitative dynamic contrast enhanced MRI of recurrent pelvic masses in patients treated for cancer. *Br J Radiol* 1998, **71**, 1136–1142.
88. Blomqvist L, Fransson P, Hindmarsh T. The pelvis after surgery and radio-chemotherapy for rectal cancer studied with Gd-DTPA-enhanced fast dynamic MR imaging. *Eur Radiol* 1998, **8**, 781–787.
89. Reddick WE, Taylor JS, Fletcher BD. Dynamic MR imaging (DEMRI) of microcirculation in bone sarcoma. *J Magn Reson Imaging* 1999, **10**, 277–285.
90. van der Woude HJ, Bloem JL, Verstraete KL, Taminiau AH, Nooy MA, Hogendoorn PC. Osteosarcoma and Ewing's sarcoma after neoadjuvant chemotherapy: value of dynamic MR imaging in detecting viable tumor before surgery. *Am J Roentgenol* 1995, **165**, 593–598.
91. Knopp MV, Brix G, Junkermann HJ, Sinn HP. MR mammography with pharmacokinetic mapping for monitoring of breast cancer treatment during neoadjuvant therapy. *Magn Reson Imaging Clin N Am* 1994, **2**, 633–658.
92. Barentsz JO, Berger-Hartog O, Witjes JA, *et al*. Evaluation of chemotherapy in advanced urinary bladder cancer with fast dynamic contrast-enhanced MR imaging. *Radiology* 1998, **207**, 791–797.
93. Padhani AR, Hayes C, Assersohn L, Powles T, Leach MO, Husband JE. Response of breast carcinoma to chemotherapy—MR permeability changes using histogram analysis. Proc. Soc. Magn. Reson. Med. 8th Scientific Meeting, Colorado, 2000.
94. de Vries A, Griebel J, Kremser C, *et al*. Monitoring of tumor microcirculation during fractionated radiation therapy in patients with rectal carcinoma: preliminary results and implications for therapy. *Radiology* 2000, **217**, 385–391.
95. Mayr NA, Yuh WT, Arnholt JC, *et al*. Pixel analysis of MR perfusion imaging in predicting radiation therapy outcome in cervical cancer. *J Magn Reson Imaging* 2000, **12**, 1027–1033.
96. Padhani AR, MacVicar AD, Gapinski CJ, *et al*. Effects of androgen deprivation on prostatic morphology and vascular permeability evaluated with MR imaging. *Radiology* 2001, **218**, 365–374.
97. Li W, Brophy DP, Chen Q, *et al*. Semiquantitative assessment of uterine perfusion using first pass dynamic contrast-enhanced MR imaging for patients treated with uterine fibroid embolization. *J Magn Reson Imaging* 2000, **12**, 1004–1008.
98. Padhani AR, O'Donell A, Hayes C, *et al*. Dynamic contrast enhanced MR imaging in the evaluation of antiangiogenesis therapy. Molecular targets and cancer therapeutics: discovery, development and cancer therapeutics. The Joint AACR-NCI-EORTC Meeting, Washington 1999. *Clin Cancer Res* 1999, **5**, 3828S.
99. Galbraith SM, Lodge M, Taylor NJ, *et al*. Combretastatin A4 phosphate reduces tumour blood flow in animal and man, demonstrated by MRI. *Proc Am Soc Clin Oncol* 2001, **20**, A279.
100. Brasch R, Pham C, Shames D, *et al*. Assessing tumor angiogenesis using macromolecular MR imaging contrast media. *J Magn Reson Imaging* 1997, **7**, 68–74.
101. Gerlowski LE, Jain RK. Microvascular permeability of normal and neoplastic tissues. *Microvasc Res* 1986, **31**, 288–305.
102. Jain R. Transport of molecules across tumor vasculature. *Cancer Metastasis Rev* 1987, **6**, 559–593.
103. van Dijke C, Brasch R, Roberts T, *et al*. Mammary carcinoma model: correlation of macromolecular contrast enhanced MR imaging characterizations of tumor microvasculature and histologic capillary density. *Radiology* 1996, **198**, 813–818.
104. Turetschek K, Huber S, Floyd E, *et al*. MR imaging characterization of microvessels in experimental breast tumors by using a particulate contrast agent with histopathologic correlation. *Radiology* 2001, **218**, 562–569.
105. Ogawa S, Menon RS, Kim SG, *et al*. On the characteristics of functional magnetic resonance imaging of the brain. *Annu Rev Biophys Biomol Struct* 1998, **27**, 447–474.
106. Abramovitch R, Frenkiel D, Neeman M. Analysis of subcutaneous angiogenesis by gradient echo magnetic resonance imaging. *Magn Reson Med* 1998, **39**, 813–824.
107. van Zijl PC, Eleff SM, Ulatowski JA, *et al*. Quantitative assessment of blood flow, blood volume and blood oxygenation effects in functional magnetic resonance imaging. *Nat Med* 1998, **4**, 159–167.
108. Robinson SP, Collingridge DR, Howe FA, Rodrigues LM, Chaplin DJ, Griffiths JR. Tumour response to hypercapnia and hyperoxia monitored by FLOOD magnetic resonance imaging. *NMR Biomed* 1999, **12**, 98–106.
109. Taylor NJ, Baddeley H, Goodchild H, *et al*. BOLD MRI of huam tumour oxygenation during carbogen breathing. *J Magn Reson Imaging* 2001, **14**, 156–163.